Numerical simulation of turbulent flow over the flat plate with shock-wave generators

Egorov Ivan and Palchekovskaya Natalia ***
** Central Aerohydrodynamic institute*
1 Zhukovsky street, Zhukovsky, Moscow region, Russia
*** Central Aerohydrodynamic institute*
1 Zhukovsky street, Zhukovsky, Moscow region, Russia

Abstract

The main part of this work is numerical investigation of shock wave interaction with turbulent boundary layer on the blunted flat plate at supersonic Mach number and high Reynolds number. For comparison, numerical simulation is also fulfilled for the sharp flat plate. Calculations are carried out using parameters of experiment in the shock tube. Two three-dimensional problems for shock wave generation by wedges, installed on the flat plate, are numerically simulated on basis of RANS equations and q-ω turbulence model. Obtained results for various values of the flat plate bluntness radius and the wedge angle satisfactorily agree with experimental data.

1. Introduction

The problem of shock wave interaction with boundary layer originated from developing of odd-shaped supersonic vehicles. Investigation of such complicated phenomena is very important for various practical applications, since local heat flux “peaks” arise in interaction regions, which complicate problem of thermal protection of the surface from aerodynamic heating. This phenomenon is generally studied using model problems, related to supersonic flow over simple geometries. One of such bodies is a flat plate, which simulates a thin lifting surface. Two kinds of interaction problems are considered for the flat plate. The first one is interaction of incident shock wave with boundary layer on the flat plate; it is usually solved in two-dimensional approach with regard to oblique shock wave. The second problem is interaction of boundary layer with shock wave, which is generated by cylindrical body or bodies, placed on the flat plate surface. This problem is a three-dimensional, and possibilities of its numerical simulation depend on capabilities of computational aerodynamics and computer technology.

Currently, in connection with requirements of applied aerodynamics, sharpened wedges are used for crossed shock waves generation. At the same time according to results of experiments and calculations (e.g. [1, 2]) the flat plate leading edge bluntness substantially influences heat exchange in the region of shock incidence and there is a threshold value of the bluntness radius r*, above which it almost has no effect on the maximum of heat transfer coefficient.

In this work interaction problems where shock wave is generated by one wedge (asymmetrical problem) and two wedges (symmetric problem) are studied.

2. The problem statement

Numerical simulation of the perfect gas flow is carried out on basis of unsteady Reynolds equations with assumptions of Boussinesq approach and differential q-ω turbulence model [3].

Reynolds-averaged Navier-Stokes equations with q-ω turbulence model in arbitrary curvilinear coordinate system (ξ,η,ζ), where $x = x(\xi,\eta,\zeta)$, $y = y(\xi,\eta,\zeta)$, $z = z(\xi,\eta,\zeta)$ - Cartesian coordinates, are written in divergence

form [4, 5].

$$\frac{\partial \mathbf{Q}}{\partial t}+\frac{\partial \mathbf{E}}{\partial \xi}+\frac{\partial \mathbf{G}}{\partial \eta}+\frac{\partial \mathbf{F}}{\partial \zeta}=\mathbf{S} \quad (1)$$

Here $\mathbf{Q}$ - vector of conservative dependent variables, $\mathbf{E}$, $\mathbf{G}$, $\mathbf{F}$ - flux vectors in curvilinear coordinate system, $\mathbf{S}$ - source vector.

Model for studying interaction problem is a flat plate of length L = 319 mm and width W = 150 mm (Figure 1). Sharp wedge of thickness b = 25 or 37.5 mm is installed on the flat plate, its leading edge is located at distance X_o = 129 mm from sharp leading edge of the flat plate.

In Figure 1 Cartesian coordinate system is indicated, which is used in analysis of computational results: coordinate system (x, y, z), point of origin is located on the plate leading edge in symmetry plane, x axis is directed along the flat plate downstream, y axis – normal to the flat plate surface, z axis is directed along leading edge of the flat plate.

Length of the flat plate L = 319 mm is taken as characteristic linear dimension and Reynolds number is calculated using this parameter and free stream values $\mathrm{Re}_L = LV_\infty \rho_\infty / \mu_\infty$.

Results of experimental investigation indicate that flow in the near-wedge region (region 2, $x > X_o$) has negligible effect on flow in the region before the wedge (region 1, $x < X_o$). Flow in the region 1 is a two-dimensional flow over the flat plate, which can be calculated independently of the region 2 in order to save computational resources. Calculation of flow over a plate, length of which is greater than X_o, gives profiles of gas-dynamic variables in section $x = X_o$. They are used as inlet boundary conditions for the computational region 2.

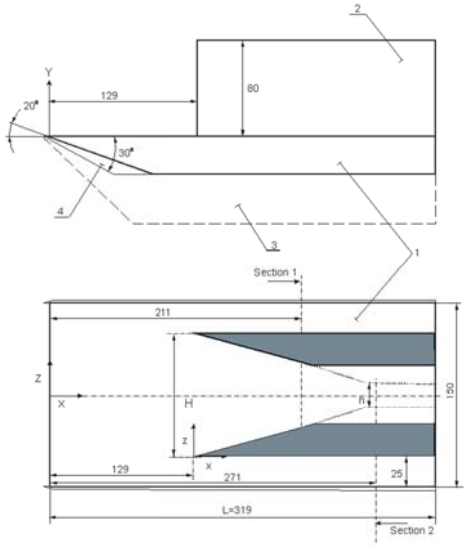

Figure 1: Scheme of the model: side view and top view

In computational region 1 simple two-dimensional grid is used. Configuration of computational region 2 depends on arrangement of wedges on the flat plate.

If only one left wedge is installed on the plate (asymmetrical problem), computational domain is chosen as follows: in direction of z axis – from the wedge surface to the symmetry plane. If two wedges are installed on the flat plate (see Figure 1) in such a way that flow field is symmetrical, in this case problem is solved for one half of flow field and three-dimensional one block grid size of 81×71×61 cells is generated. For this domain boundaries are chosen as follows: in direction of z axis – from the wedge surface to the middle of the flat plate, and in direction of x axis – from the wedge leading edge to the end of the flat plate.

Interaction of shock wave with boundary layers on sharp and blunted flat plates numerically investigated on basis of equations for viscous perfect gas dynamics. Calculations are carried out at parameters, corresponding to the experimental ones: Mach number M_∞ = 5; stagnation pressure p_o = 69 bar; stagnation temperature T_o = 530 K;

Reynolds number $Re_{\infty L} = 27 \cdot 10^6$.
In numerical simulation it is assumed that moving medium is a perfect gas with $\gamma = 1.4$, Pr = 0.7 and dynamic viscosity coefficient, depending on temperature according to Sutherland law.
Bluntness radius of the flat plate takes the following values: r* = 0 and 0.75 mm (r = r* / L = 0 and 0.00235).
Wedges with sharp leading edge and angles of flow inclination $\theta_w = 10^\circ$, 15° and 20° are considered. It is assumed that surfaces are isothermal with temperature factor $T_{wo} = T_w/T_o = 0.57$.

3. Asymmetrical problem

Interaction of boundary layer on the flat plate with shock waves, which are generated by wedges, installed on the plate, is a three-dimensional problem and it is simulated using three dimensional equations for perfect viscous gas dynamics.

Comparison of numerical and experimental fields of pressure coefficient c_p on the flat plate surface (Figure 2) shows good agreement of these results.

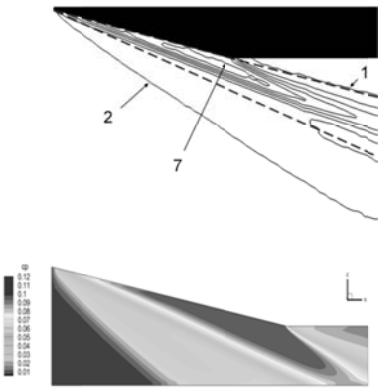

Figure 2: Numerical and experimental fields of pressure coefficient on the flat plate with one wedge: $\theta_w = 10^o$, $M_\infty = 5$, $Re_{\infty L} = 27 \cdot 10^6$: laminar-turbulent flow. Top picture – experiment, bottom – numerical computation. Dashed lines show location of shock wave (inviscid solution) and spreading line. Isobars: 1 - $c_p = 0$, 2 – $c_p = 0.045$, 7 – $c_p = 0.27$.

Problem of flow over the finite-length plate with one (left) wedge describes transitional flow from disturbed by the wedge to uniform flow at zero pressure gradient. In inviscid gas flow over a wedge spatial stream with linear boundaries between various flow regions is realized. In viscid flow linearity of boundaries approximately maintains in the first half of the computational domain.
Before blunted flat plate curvilinear bow shock wave is generated. The plate has two characteristic linear scales: L – length of the plate, L = 319 mm and r – bluntness radius of the plate leading edge r* = 0 and 0.75 mm (r = r*/L = 0 and 0.00235).
Fields of pressure coefficient c_p and isolines pattern c_p = const for sharp and blunted plates with one wedge show complex structure of disturbed flow field (Figure 3).
In pressure coefficient c_p field five characteristic flow regions are denoted by corresponding number (see Figure 3a).

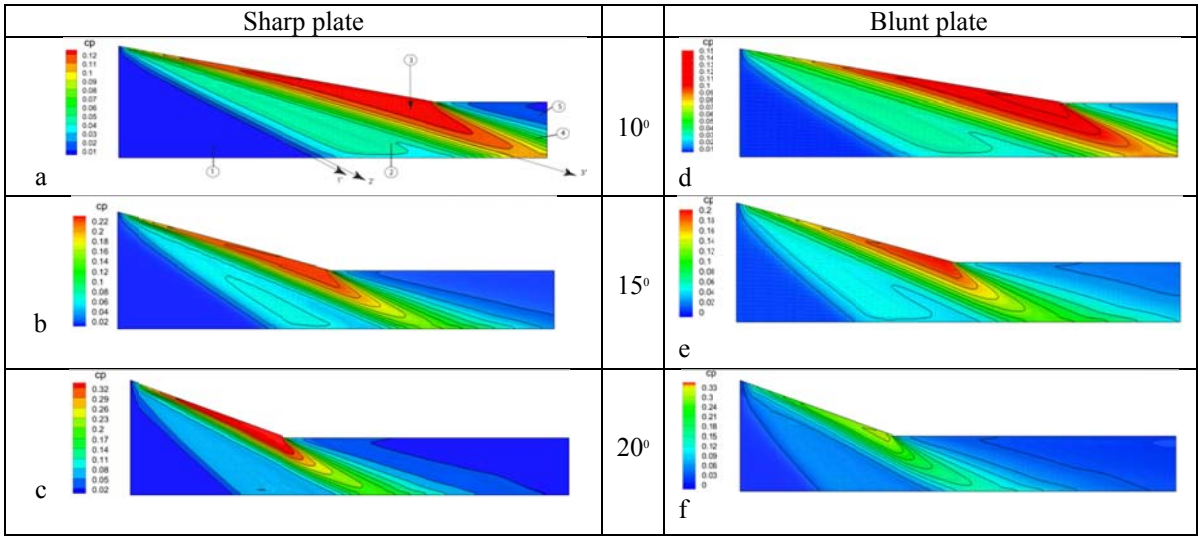

Figure 3: Numerical and experimental fields of pressure coefficient on the flat plate with one wedge: $\theta_w = 10^o$,

In region 1 ($c_p \approx 0.015$) flow at zero pressure gradient is realized. The region 2 consists of two layers: layer 1′ ($c_p \approx 0.015$) – narrow strip with low friction stress, where bow shock wave interacts with boundary layer, and layer 2′ ($c_p \approx 0.05$) – strip of quasi-inviscid flow (close to the uniform one). The region 3 ($c_p \approx 0.115$) – region of wall viscous flow; in this region zones with maximum value of pressure coefficient are observed. In the region 4 ($c_p \approx 0.07$) flow turns around (rarefaction fan) near the corner point of the wedge. The region 5 ($c_p \approx 0.01$) is a region of circulation flow, where gas flow in and flow out from outside; as a result the main leaked-in flow is driven back from the surface in vicinity of the corner point, which is streamlined without separation.

In Figure 4 patterns of friction coefficient are presented.

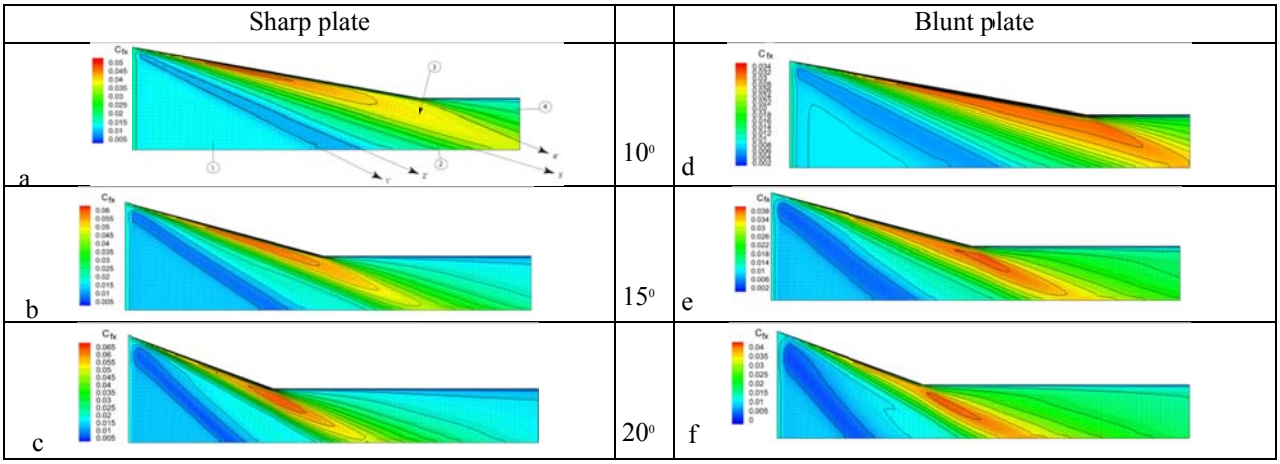

Figure 4: Fields of friction coefficient $c_{f\,x}$ and isolines of c_{fx} for sharp (a, b, c) and blunt (d, e, f) flat plate with one wedge

Within the bounds of asymptotic approach longitudinal component c_{fx} is an internal solution and corresponds to forces of viscous friction at given pressure field. Because of this fact fields of c_{fx} differ from corresponding results for pressure coefficient, but at the same time they confirm community in structure of field patterns under consideration. The main quality difference between them is following. If pressure coefficient field is divided into five regions (Figure 3a), field c_{fx} is divided only into four flow regions (Figure 4a). The region 1 ($c_{fx} \approx 0.01$) – region of flow at zero pressure gradient. The region 2 consist of two layers: layer 1′ - zone of bow shock and boundary layer interaction ($c_{fx} \approx 0.005$), layer 2′ - strip of quasi-inviscid flow (close to uniform) ($c_{fx} \approx 0.03$). The region 3 – wall viscous layer ($c_{fx} \approx 0.045$). The region 4 – zone of outlet flow ($c_{fx} \approx 0.03$).

In Figure 5 distribution of friction coefficient along longitudinal coordinate in section $z = 0$ is shown. For sharp plate there is a high level of c_{fx}, which can achieve values $0.05 \div 0.065$; bluntness of the plate leading edge arouses its appreciable drop - $c_{fx} \approx 0.034 \div 0.04$. In the region 1 value of c_{fx} is nearly constant and continuously moves to the layer 1′ of region 2; in this layer c_{fx} takes low positive values and it means that there is no flow separation in the layer 1′. The region 2 for $\theta_w = 10^\circ$ spreads along longitudinal coordinate nearly whole space in this section. Further behavior of function $c_{fx} = c_{fx}(x)$ demonstrate features of flow development at $\theta_w = \text{const}$. For $\theta_w = 10^\circ$ it is a monotone increasing function with inflection point, and for other wedge angle it consist of two branches – ascending and descending. On the ascending branch "plateau" is formed, that is correspond to the layer 2′ with quasi-inviscid flow and contains local maximum and minimum; it indicates formation of local flow relaminarization region.

For the blunted plate friction stress is lower. At this conditions flow in layer 1′ of region 2 has no separation, and friction coefficient in this zone achieves the minimum value $c_{fx,min}$. Using linear approximation of dependence $c_{fx,min} = c_{fx,min}(\theta_w)$, it is possible to estimate angle θ_w, at which flow separates in longitudinal direction. Calculations show that for sharp and blunt plates separation arises at the same angle $\theta_w \approx 30^\circ$.

In Figure 6 distribution of the maximum Stanton number St_m in middle section along longitudinal coordinate is presented.

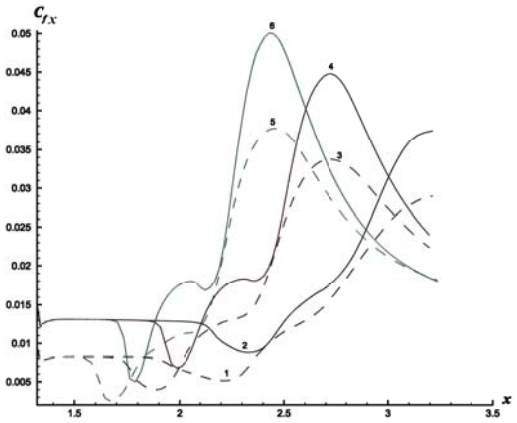

Figure 5: Distribution of friction coefficient c_{fx} in middle section of the plate with one wedge ($M_\infty = 5$, $Re_{\infty L} = 27 \cdot 10^6$): 1, 3, 5 – blunted plate (r = 0.75 mm), 2, 4, 6 – sharp plate (r = 0), 1, 2 – $\theta_w = 10^\circ$, 3, 4 – $\theta_w = 15^\circ$, 5, 6 – $\theta_w = 20^\circ$; x coordinate is in dm

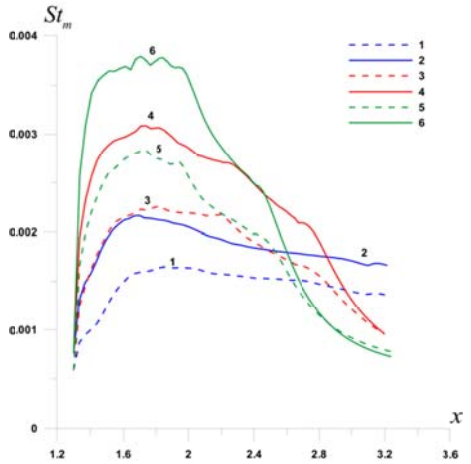

Figure 6: Distribution of maximum Stanton number St_m in middle section of the plate with one wedge ($M_\infty = 5$, $Re_{\infty L} = 27 \cdot 10^6$): 1, 3, 5 – blunt plate (r = 0.75 mm), 2, 4, 6 – sharp plate (r = 0), 1, 2 – $\theta_w = 10^\circ$, 3, 4 – $\theta_w = 15^\circ$, 5, 6 – $\theta_w = 20^\circ$

Stanton number St_m varies in longitudinal direction in unmonotonic way and influenced by angle θ_w and bluntness radius r_*.

3. Symmetrical problem

In Figure 7 fields of pressure coefficient on the plate surface are presented. It is seen that in comparison with one wedge case structure of flow field becomes more complex. According to Figure 7 wedge angle has strong effect on structure of pressure coefficient field, which qualitatively and quantitatively changes with θ_w increase. Comparison of pressure coefficient fields for sharp plates with $\theta_w = 10^o$ (Figure 7a) and 15^o (Figure 7b) shows that in both cases oblique shock reflects from the symmetry plane in a regular way. In the first case reflected shock goes beyond the computational domain, and in the second case it reaches wedge surface, reflects from it and after that leaves the computational domain.

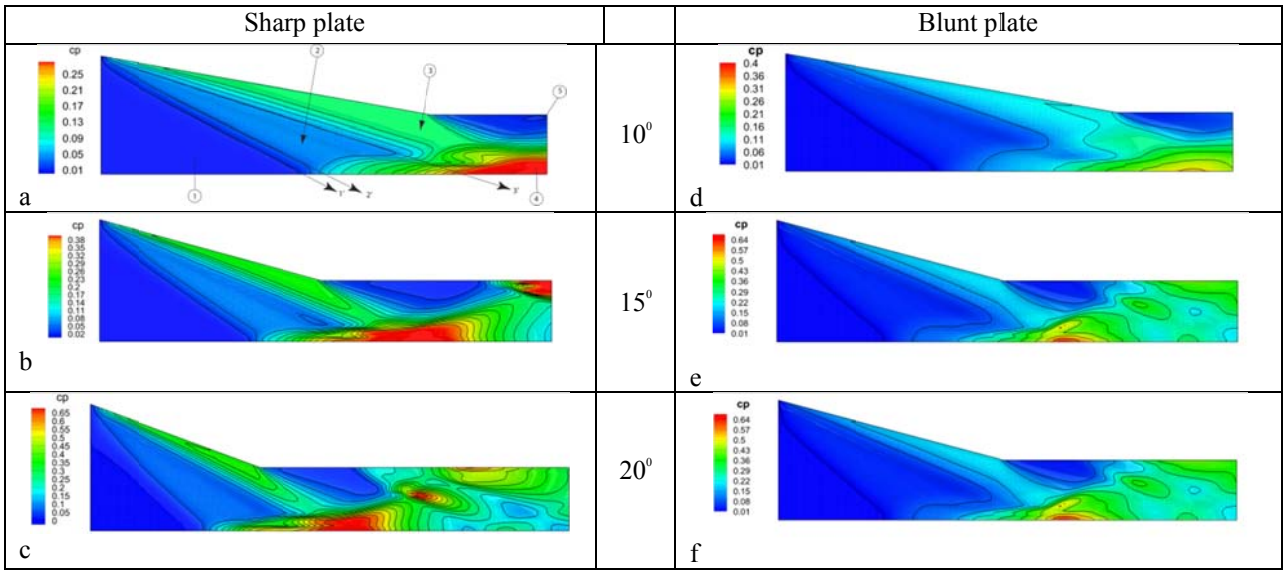

Figure 7: Fields of pressure coefficient c_p and isolines c_p = const for sharp (a, b, c) and blunt (d, e, f) flat plates with two wedges

Differences in c_p fields for plates with wedge angles $\theta_w = 15^o$ (Figure 7b) and 20^o (Figure 7c) are quantitative and related to changes in geometry of the computational domain. For example, zone of reflected shock interaction with the wedge surface is formed in the vicinity of the outflow boundary of the computational domain. In the first case it is partially situated within the computational domain and in the second case it is fully inside it.

In patterns of cp various zones with nearly constant pressure coefficient value can be marked out. In case of the plate with 10^o wedges (Figure 7a) structure c_p of field is the simplest – it has five zones.

Zone 1 (between leading edge and ray 1′) – zone of flow without gradient ($c_p \approx 0.01$). This zone corresponds to region of unperturbed flow.

Zone 2 ($c_p \approx 0.05$) between rays 1′ and 3′ contains two regions: region between rays 1′ and 2′, where bow shock interacts with boundary layer on the plate, and region between rays 2′ and 3′, corresponding to the region of quasi-inviscid flow behind the bow shock. Zone 3 ($c_p \approx 0.13$) has complicated configuration: it reproduces characteristic elements of flow field structure when shock reflecting from the symmetry plane. Zones 4 ($c_p \approx 0.23$) and 5 ($c_p \approx 0.01$) are open zones of global separation. In comparison with the one-wedge flat plate in flow field concerned two additional processes take place – interaction in zone of shock incidence and reflection from symmetry plane and interaction of entropy layer, generated by small bluntness, with boundary layer.
Flow over the plate with two wedges has complex structure, which involves regions and zones of different scales

with linear and curvilinear boundaries.
In Figure 8 fields of friction coefficient are presented, where following zones can be marked out. Zone 1 - zone of flow without gradient (between leading edge and ray 1′). Zone 2 – zone between rays 1′ and 2′, corresponding to bow shock interaction with boundary layer on the plate; zone 3 between rays 2′ and 3′, corresponding to flow region with monotone increase of local friction stress. Zone 4 has complex shape, reproducing process of supersonic flow reflection from the symmetry plane. Zones 5 and 6 are located on the boundary of computational domain, through which gas flows from outside to the computational domain.

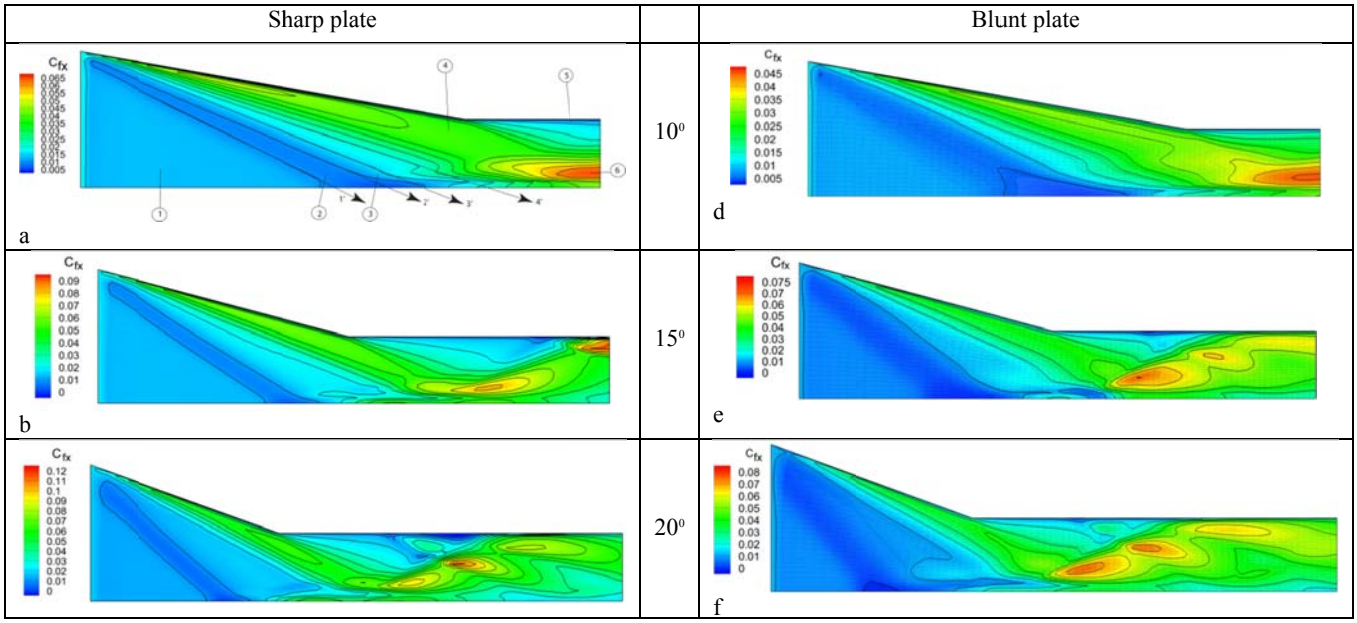

Figure 8: Fields of friction coefficient $c_{f\,x}$ and isolines c_{fx} =const for sharp (a, b, c) and blunt (d, e, f) flat plate with two wedges

In Figure 9 distributions of local aerodynamic characteristics are presented. For the regimes concerned pressure coefficient is positive ($c_p > 0$). Longitudinal component of friction coefficient is a positive function, excepting three computational regimes (sharp plate at $\theta_w = 20^\circ$ and blunt plate at $\theta_w = 15^\circ$ and 20°), and corresponds to flow without separation. Heat flux is a positive function and takes on constant value in flow regions, where separation arises.
Given dependencies have two branches – ascending and descending. Behavior of aerodynamic characteristics suggests laminar-turbulent flow over the flat plate. Formation of "plateau" in pressure coefficient distribution and double-peak distributions of friction coefficient and heat flux in zone of their maxima indicate occurrence of relaminarization regions with following flow turbulization. Sizes of these regions growth with increase of wedge angle. For the blunt plate values of the parameters concerned less than for the sharp one.
Bluntness of the flat plate leads to following decrease of maximum values: max c_p – 1.6 times less, max c_{fx} – 1.7 times less, max q^o – 1.4 times less. From the data given it follows that small bluntness of the plate leading edge leads to substantial decrease of maximum pressure and friction coefficients and maximum heat flux in the interaction region. Decrease of maxima occurs on the same level for all quantities and is accompanied by shift of main maxima position upstream. It should be noted that presence of small bluntness makes heat flux distribution smoother, i.e. maximum values of temperature gradients decrease.

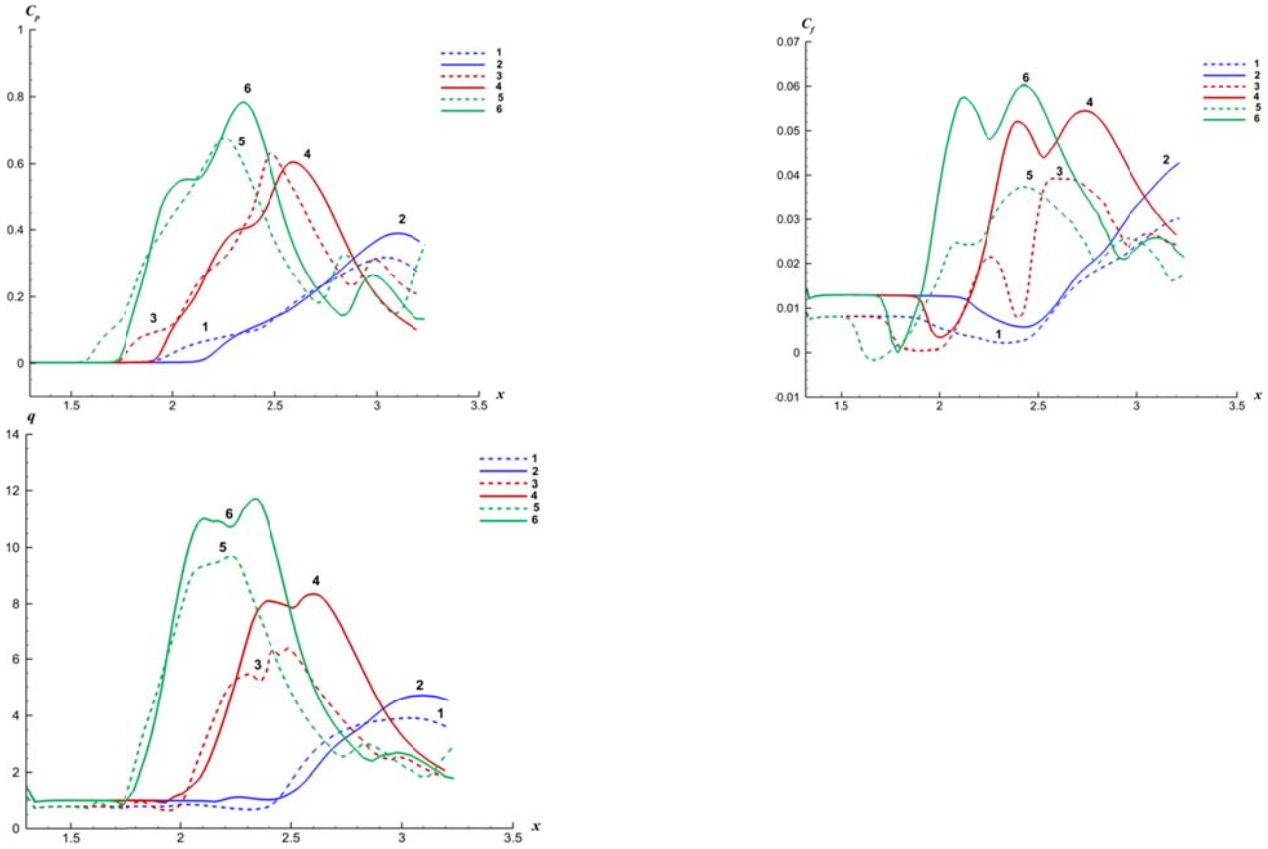

Figure 9: Distribution of pressure coefficient (a), friction coefficient (b) and heat flux (c) along the flat plate in symmetry plane ($M_\infty = 5$, $Re_{\infty L} = 27 \cdot 10^6$): 1, 3, 5 – blunt plate (r = 0.75 mm), 2, 4, 6 – sharp plate (r = 0), 1, 2 – $\theta_w = 10^o$, 3, **4** – $\theta_w = 15^o$, 5, 6 – $\theta_w = 20^o$

In Figure 10 behaviour of maximum Stanton number St_m on the plate surface is presented.

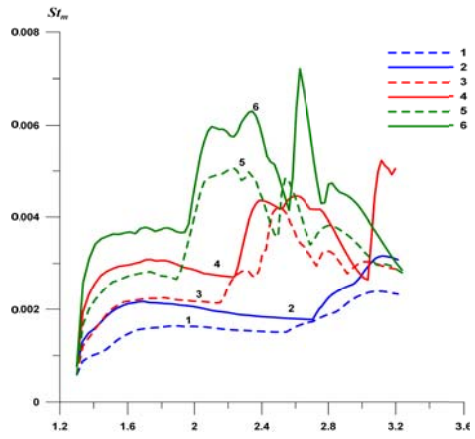

Figure 10: Distribution of maximum Stanton number St_m in symmetry plane of the plate with two wedges ($M_\infty = 5$, $Re_{\infty L} = 27 \cdot 10^6$): 1, 3, 5 – blunt plate(r = 0.75 mm), 2, 4, 6 – sharp plate (r = 0), 1, 2 – $\theta_w = 10^o$, 3, 4 – $\theta_w = 15^o$, 5, 6 – $\theta_w = 20^o$

4. Conclusion

Interaction of shock wave with laminar and turbulent boundary layers on sharp an blunt flat plates at supersonic Mach number ($M_\infty = 5$) and high Reynolds number ($Re_{\infty L} \leq 27 \cdot 10^6$). On basis of Reynolds equations and q-ω turbulence model two three-dimensional problems for shock generation by wedges are numerically simulated. Numerical results are obtained for various values of bluntness radius (r = 0 and r = 0.75 mm) and wedge angle ($\theta_w = 10^o, 15^o, 20^o$). These results satisfactory agree with experimental data.

According to numerical results incorrect solution in small neighbourhood of sharp leading edge similar to case with small bluntness, in particular, induces weak bow shock, which participates in interaction process. In this case sharp and blunt plates have one-type structures of flow fields. Quantitative differences take place because of different values of effective bluntness radius.

Small bluntness of the plate leading edge substantially reduces maximum values of heat transfer coefficient (St_m) and pressure coefficient in the interaction zone; at the same time zone of enhanced heat exchange and high pressure broadens. These features of flow field are related to generation of detached shock wave and thin entropy layer near the blunt plate. Existence of threshold value of bluntness radius r* is also confirmed.

References

[1] Borovoy V. Ya., Egorov I. V., Skuratov A. S.,Struminskaya I. V.(2011). Two-dimensional interaction of the oblique shock wave with the boundary and high-entropy layers of the blunt plate. *AIAA* 2011-731.

[2] Borovoy, V. Ya., Egorov, I. V., Skuratov, A. S., and Struminskaya, I. V. (2005). Interaction between an inclined shock and boundary and high-entropy layers on a flat plate. *Fluid Dynamics*. 40(6):911–928.

[3] Huang, P. G., Coakley, T. J. (1992). Turbulence modeling for high speed flows. *AIAA Paper*. 92-0436.

[4] Bashkin, V.A. and Egorov, I.V. (2012). Numerical simulation of prefect viscous gas flow, Moscow: Fizmatlit, 372 p. (in Russian).

[5] Bashkin, V.A. and Egorov, I.V. (2013). Numerical simulation of internal and external aerodynamics problems, Moscow: Fizmatlit, 332 p. (in Russian).